

Article

Highly Selective Nitrogen-Doped Graphene Quantum Dots/Eriochrome Cyanine Composite Photocatalyst for NADH Regeneration and Coupling of Benzylamine in Aerobic Condition under Solar Light

Ruchi Singh ¹, Rajesh K. Yadav ^{1,*}, Ravindra K. Shukla ¹, Satyam Singh ¹, Atul P. Singh ², Dilip K. Dwivedi ³, Ahmad Umar ^{4,5,*}  and Navneet K. Gupta ⁶ 

¹ Department of Chemistry and Environmental Science, Madan Mohan Malviya University of Technology, Gorakhpur 273010, India

² Department of Chemistry, Chandigarh University Mohali, Mohali 140413, India

³ Department of Physics and Materials Science, Madan Mohan Malaviya University of Technology, Gorakhpur 273010, India

⁴ Department of Chemistry, Faculty of Science and Arts, and Promising Centre for Sensors and Electronic Devices (PCSED), Najran University, Najran 11001, Saudi Arabia

⁵ Department of Materials Science and Engineering, The Ohio State University, Columbus, OH 43210, USA

⁶ Centre for Sustainable Technologies, IISc Bangalore Gulmohar Marg, Banglaru 560012, India

* Correspondence: rajeshkr_yadav2003@yahoo.co.in (R.K.Y.); ahmadumar786@gmail.com (A.U.)

† Adjunct Professor at the Department of Materials Science and Engineering, The Ohio State University, Columbus, OH 43210, USA.



Citation: Singh, R.; Yadav, R.K.; Shukla, R.K.; Singh, S.; Singh, A.P.; Dwivedi, D.K.; Umar, A.; Gupta, N.K. Highly Selective Nitrogen-Doped Graphene Quantum Dots/Eriochrome Cyanine Composite Photocatalyst for NADH Regeneration and Coupling of Benzylamine in Aerobic Condition under Solar Light. *Catalysts* **2023**, *13*, 199. <https://doi.org/10.3390/catal13010199>

Academic Editors: Indra Neel Pulidindi, Archana Deokar and Aharon Gedanken

Received: 2 November 2022

Revised: 28 December 2022

Accepted: 9 January 2023

Published: 14 January 2023



Copyright: © 2023 by the authors. Licensee MDPI, Basel, Switzerland. This article is an open access article distributed under the terms and conditions of the Creative Commons Attribution (CC BY) license (<https://creativecommons.org/licenses/by/4.0/>).

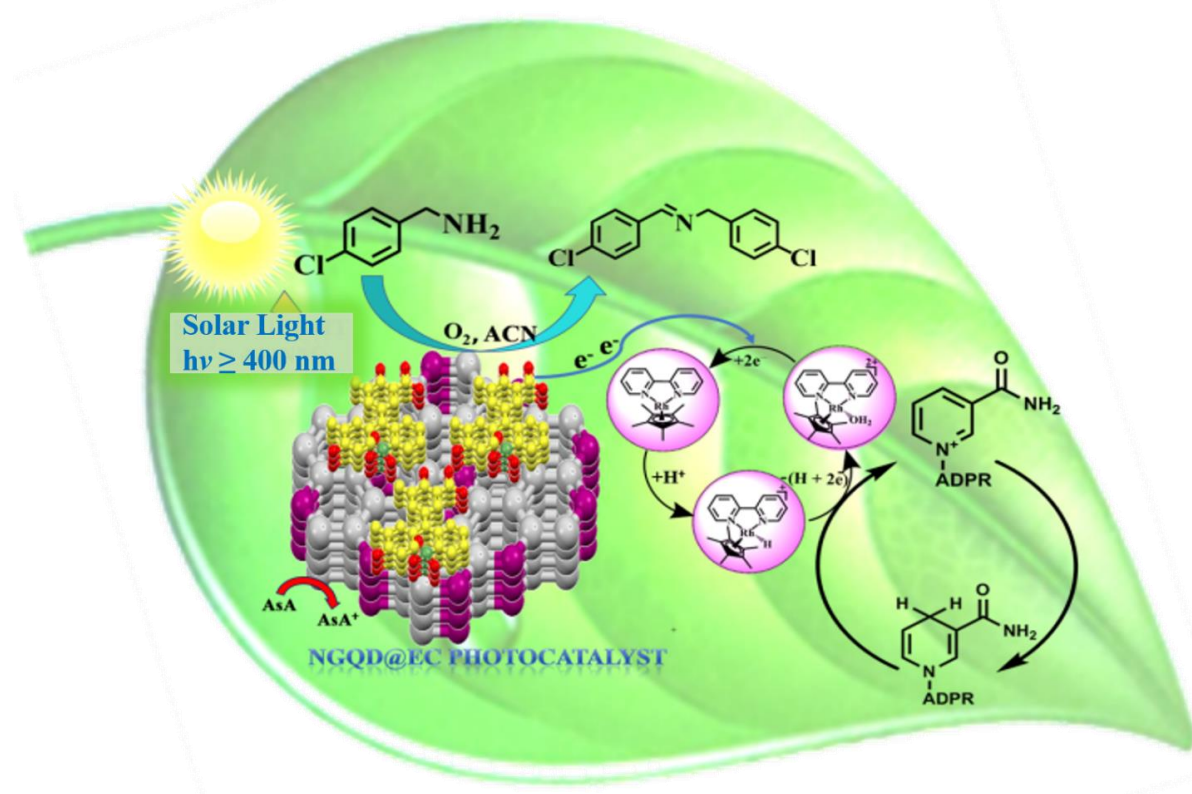
Abstract: Photocatalysis is an ecofriendly and sustainable pathway for utilizing solar energy to convert organic molecules. In this context, using solar light responsive graphene-based materials for C–N bond activation and coenzyme regeneration (nicotinamide adenine dinucleotide hydrogen; NADH) is one of the utmost important and challenging tasks in this century. Herein, we report the synthesis of nitrogen-doped graphene quantum dots (NGQDs)-eriochrome cyanine (EC) solar light active highly efficient “NGQDs@EC” composite photocatalyst for the conversion of 4-chloro benzylamine into 4-chloro benzylamine, accompanied by the regeneration of NADH from NAD⁺, respectively. The NGQDs@EC composite photocatalyst system is utilized in a highly efficient and stereospecific solar light responsive manner, leading to the conversion of imine (98.5%) and NADH regeneration (55%) in comparison to NGQDs. The present research work highlights the improvements in the use of NGQDs@EC composite photocatalyst for stereospecific NADH regeneration and conversion of imine under solar light.

Keywords: NADH regeneration; NGQDs@EC composite; Glucose; Graphene

1. Introduction

Using solar light for the conversion of sustainable resources into chemicals by mimicking natural photosynthesis is a challenge. Usages of solar light harvesting artificial photosynthesis are increasing. Due to amazing chemical, mechanical and physical properties, light-harvesting composites have attracted massive attention. These materials also show unique π -conjugated structures. Light harvesting composites are extremely useful in a variety of applications, including organic separation [1,2] gas storage [3] biocatalysis [4] etc. For the catalytic process, a range of solar light harvesting 2D graphene materials have been studied, including organic dye-based 2D graphene material [5], nitrogen-containing 2D graphene materials [6,7], and 2D graphene-based nanomaterials [8]. Among this, nitrogen-enriched graphene has attracted attention due to its solar light active photocatalytic ability [9], chemical stability, and extraordinary biocompatibility [10]. Furthermore,

bulk nitrogen-enriched graphene has the problem of easy, fast recombination of solar light-irradiated electron–hole couples [11] and allegation of inadequate solar light absorption capacity-related lighting, which ruthlessly limits the catalytic performance in the presence of solar light for the regeneration of redox-active cofactors. To date, various efforts have been made to improve either of the two aspects in order to uplift the redox-active cofactors in photocatalytic phenomena. Therefore, to enhance the photocatalytic ability of nitrogen-enriched graphene quantum dots via π – π stacking of dyes [12], we report the synthesis of NGQDs-based eriochrome cyanine (EC) solar light highly efficient, i.e., NGQDs@EC composite photocatalyst for excellent conversion of NAD⁺ (nicotinamide adenine dinucleotide) to NADH (nicotinamide adenine dinucleotide hydrogen) regeneration and coupling of benzylamine in aerobic conditions under solar lights, as shown in Scheme 1.



Scheme 1. Photocatalytic NADH regeneration and organic transformation.

2. Results and Discussion

The UV absorption studies of NGQDs and NGQDs@EC have been conducted in DMF. We evaluated the UV–visible spectra of the NGQDs composite to evaluate the optical properties of the newly generated highly selective NGQDs@EC, as shown in Figure 1a. In comparison to NGQDs, NGQDs@EC have a broad absorption peak at 576 nm in the visible region [13]. The optical band gap of NGQDs and NGQDs@EC photocatalyst are 2.32 eV and 2.15 eV, respectively. The optical band gap energy was calculated using the following equation: E_g (eV) = 1240/ λ (wavelength in nm). The covalent conjugation of melamine and glucose units (NGQDs) results in a significant increase in the absorption coefficient in the spectral window of 400 nm, allowing for a more efficient light-harvesting nature [14,15]. Figure 1b,c shows the direct and correct extrapolation approaches used to estimate the optical band gap of the synthesized photocatalysts, as shown in the tauc plots. From the tauc plots, the obtained band gap of the NGQDs@EC photocatalyst is 2.15 eV. Additionally, we compared the energy level or band gap position from the cyclic voltammetry [16]. The cyclic voltammetry (CV) experiment also confirms the same type of band gap (Figure 2a,b). As shown in Figure 2a, NGQDs@EC photocatalyst has oxidation and reduction potentials near +1.22 V and −0.88 V, respectively.

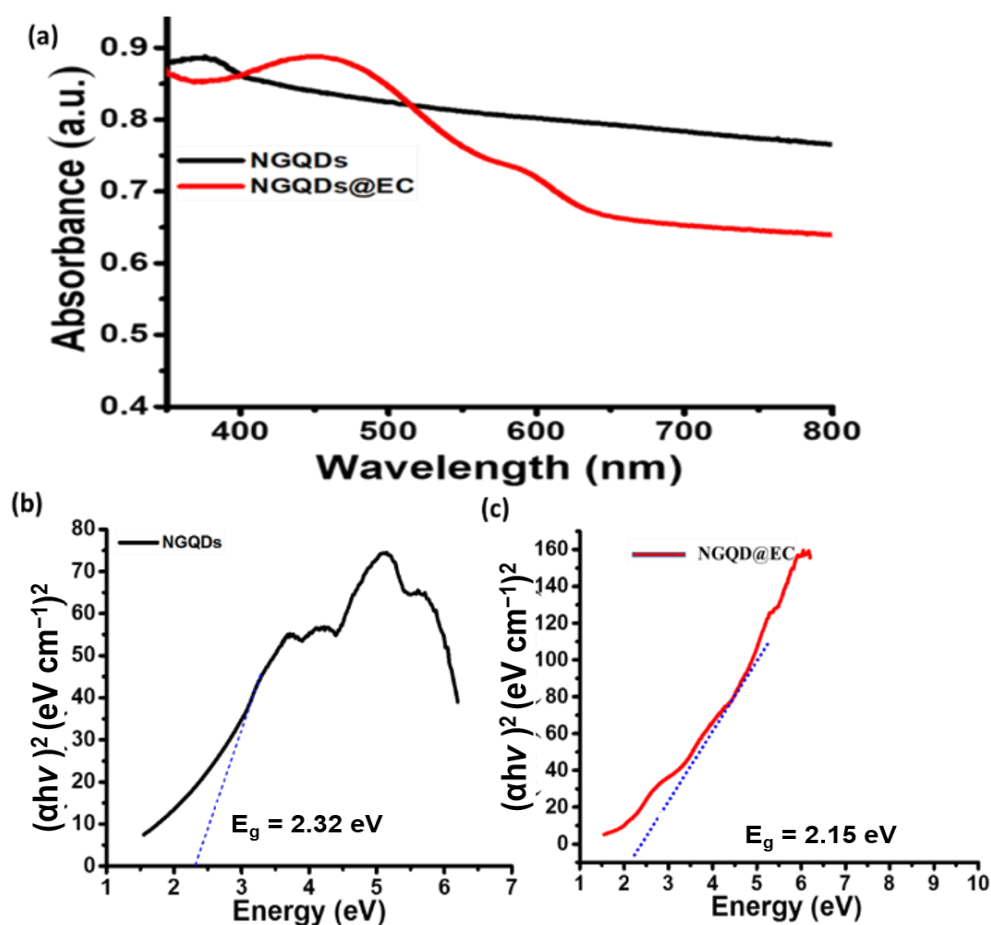


Figure 1. (a) UV-visible diffuse reflectance spectra (DRS) of NGQDs (black line) and NGQDs@EC (red line) photocatalyst, respectively, (b) Tauc plot of NGQDs, (c) Tauc plot of NGQDs@EC photocatalyst.

The collected redox potential data can be used to calculate the band gap [17]. Figure 2b shows the Latimer diagram derived from cyclic voltammetry, which confirmed the band gap of 2.10 eV, which is similar to the calculated band gap from Figure 1.

The Fourier-transform spectroscopy (FTIR) was used to identify the functional group. In Figure 3a, the FTIR spectrum of NGQDs has two main peaks: a peak centered at 1637 cm^{-1} and a broad peak at 3402 cm^{-1} , both revealing O–H bonding. Along with these, peaks at 1255 cm^{-1} and 1078 cm^{-1} indicate the existence of C–H and C–O, respectively. After the π – π stacking of EC on NGQDs, the peaks were shifted to 3100 cm^{-1} and 1092 cm^{-1} due to C–H and C–O stretching and new peaks formed at 2164 cm^{-1} [18–20]. These results clearly indicated that the EC chromophore was stacked on NGQDs via π – π stacking.

The thermal behavior of NGQDs and NGQDs@EC photocatalysts was investigated by differential scanning calorimetry (DSC, model: 2910) in Figure 3b at a heating rate of $5\text{ }^{\circ}\text{C}/\text{min}$ under N_2 flow in the temperature range from 50 to $300\text{ }^{\circ}\text{C}$. The NGQDs@EC photocatalyst has strong water adsorption effects. Figure 3b clearly indicated that the synthesized NGQD@EC photocatalyst is stable up to $225\text{ }^{\circ}\text{C}$. As well the sublimation and thermal condensation of NGQDs was observed at 50 – $140\text{ }^{\circ}\text{C}$. So, the NGQD@EC photocatalyst is more stable and more efficient than NGQDs [21].

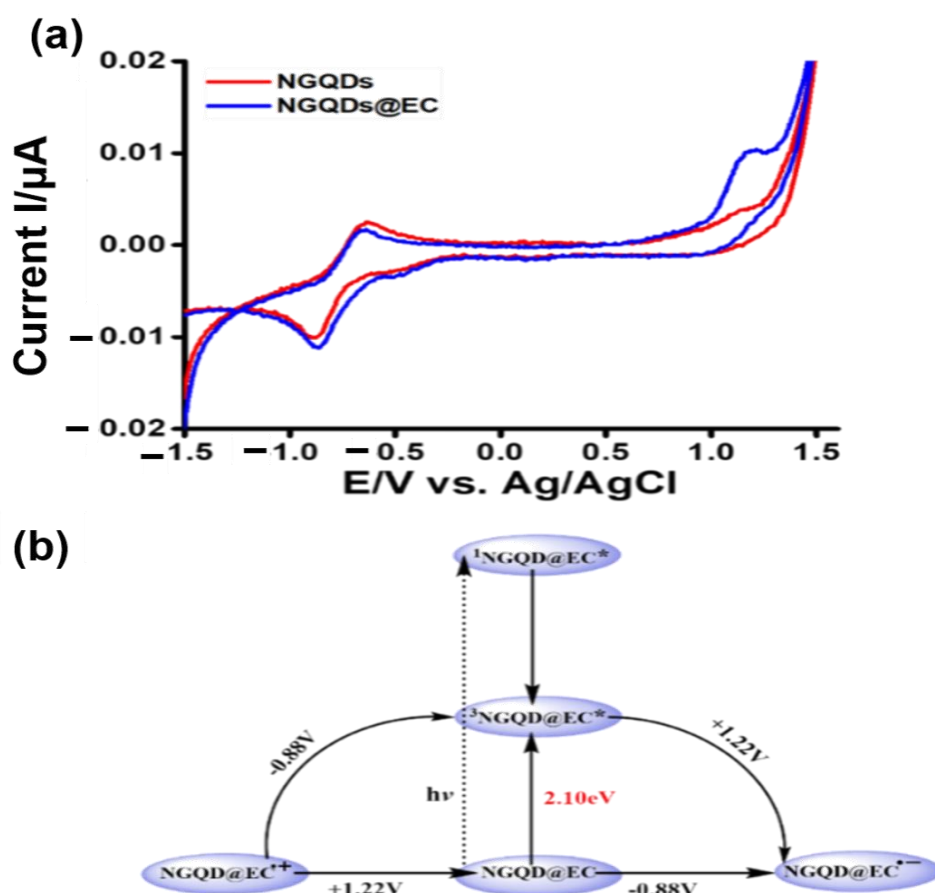


Figure 2. (a) Cyclic voltammetry (CV) of NGQDs (red line) and NGQDs@EC (blue line) photocatalyst, respectively, (b) Latimer diagram of NGQDs@EC photocatalyst.

The nature and the size of particles were investigated by X-ray diffraction pattern (XRD). Figure 4 shows the diffraction pattern of NGQDs@EC and NGQDs photocatalysts. The observed diffraction pattern exhibited few well-defined diffraction peak for NGQDs appeared at $2\theta = 11.03^\circ$, 13.07° , 21.09° , and 27.08° . Interestingly, after the π - π stacking of EC on the NGQDs, the crystalline nature of the composite was increased with a significant shift in the diffraction peaks. Thus, the observed diffraction pattern for the NGQD@EC composite show various high-intensity peaks at $2\theta = 13.1^\circ$, 20.4° , 24.32° , and 27.89° [22].

The zeta potential of NGQDs and NGQDs@EC were found to be -11.8 and -29.2 mV, as shown in Figure 5a,b respectively. In comparison to NGQDs, the NGQDs@EC photocatalyst has a higher negative zeta potential value, indicating that it is more stable. The higher chemical stability of the NGQDs@EC due to the creation of the C-N bond is likely to explain the greater negative zeta potential value when compared to the NGQDs [16,23].

2.1. The Enzymatically Active and Inactive 1,4-NADH Cofactor Regeneration

The goal of this research is to recover the enzymatically active 1,4-NADH (1,4-Nicotinamide adenine dinucleotide) cofactor from its oxidized versions, NAD^+ . The NAD^+ undergoes an unselective protonation and radical coupling reaction, as shown in Scheme 2.

Because of this process, numerous NAD isomers, both active and inactive, are produced. Using an electron mediator, you can prevent the formation of enzymatically inactive isomers. Under sunlight irradiation, the rhodium complex mediator helps to regenerate enzymatically active 1,4-NADH isomer only. At room temperature in an inert atmosphere, photochemical regenerations of 1,4-NADH cofactors were carried out under artificial sunlight irradiation ($\lambda > 420$ nm) [15,16,24].

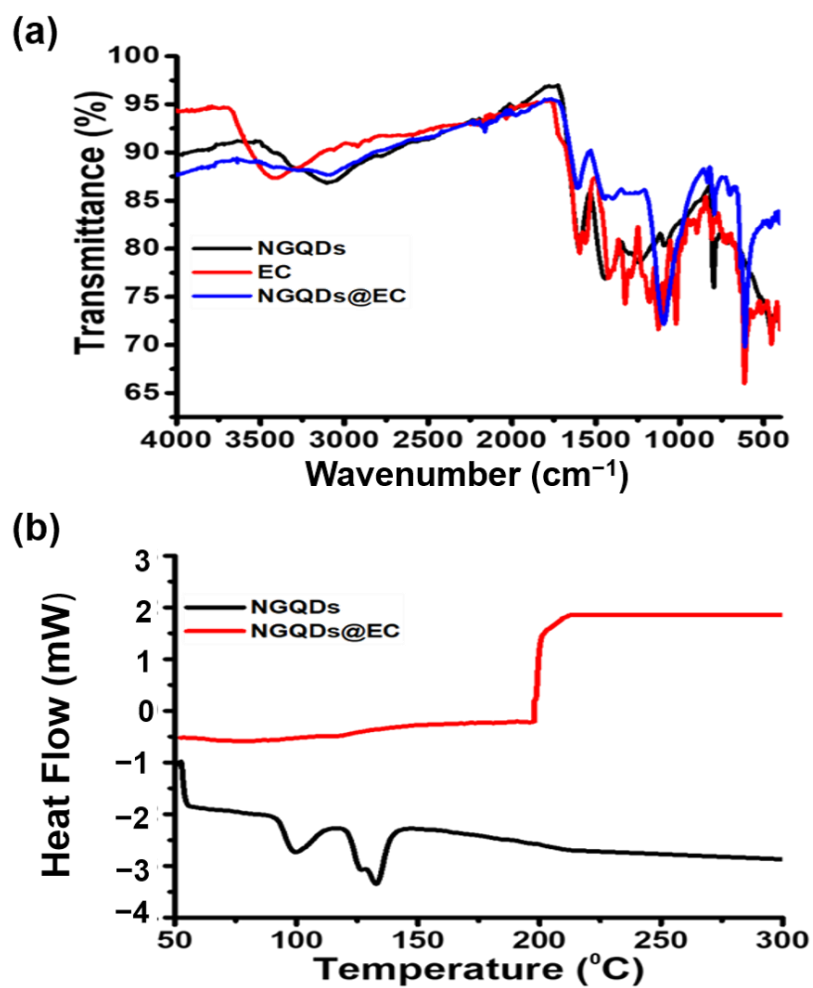


Figure 3. (a) FTIR spectra of EC (red line), NGQDs (black line), and NGQDs@EC (blue line) photocatalysts respectively, and (b) DSC of NGQDs@EC (red line) and NGQDs (black line) photocatalyst respectively.

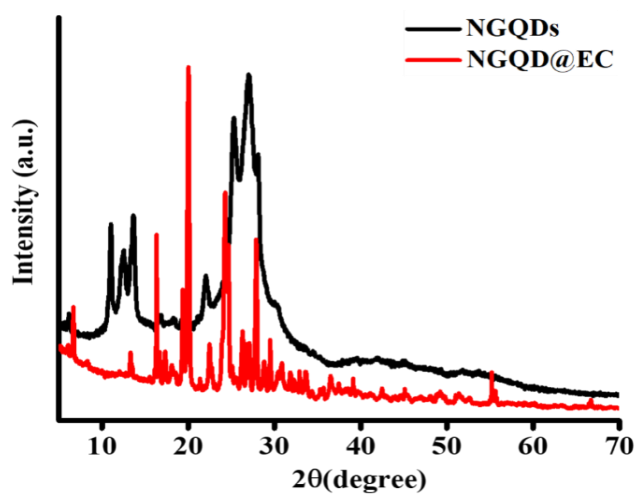


Figure 4. X-ray Diffraction pattern (XRD) of NGQDs and NGQD@EC.

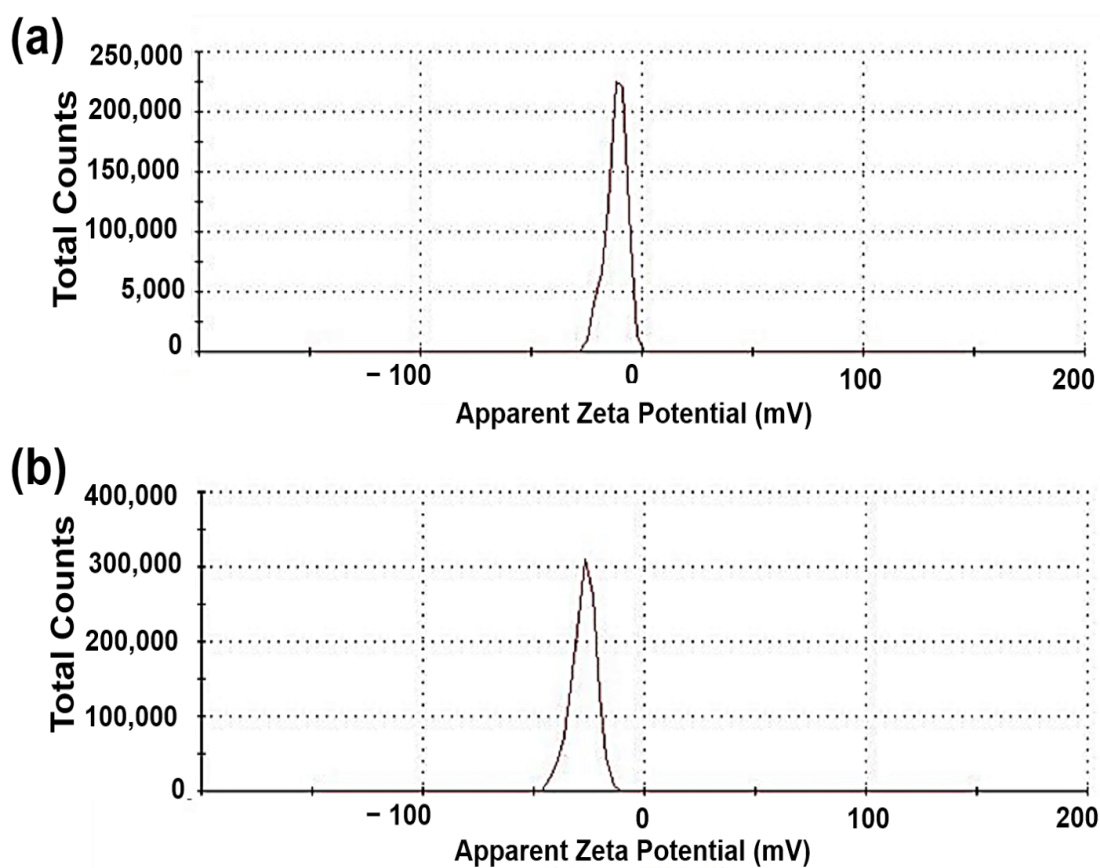
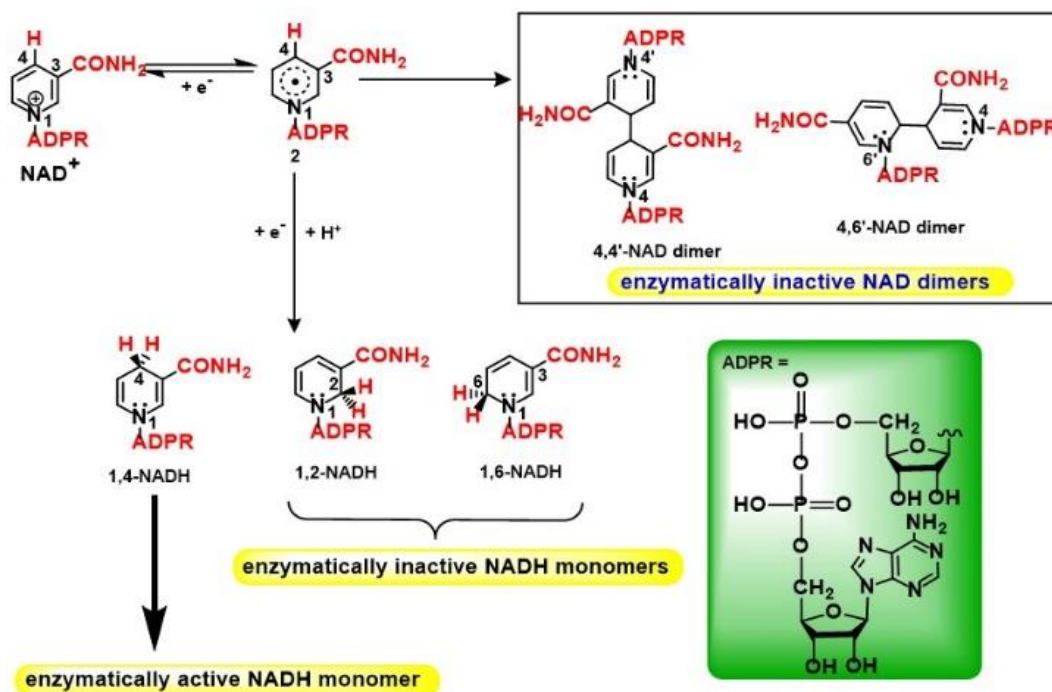


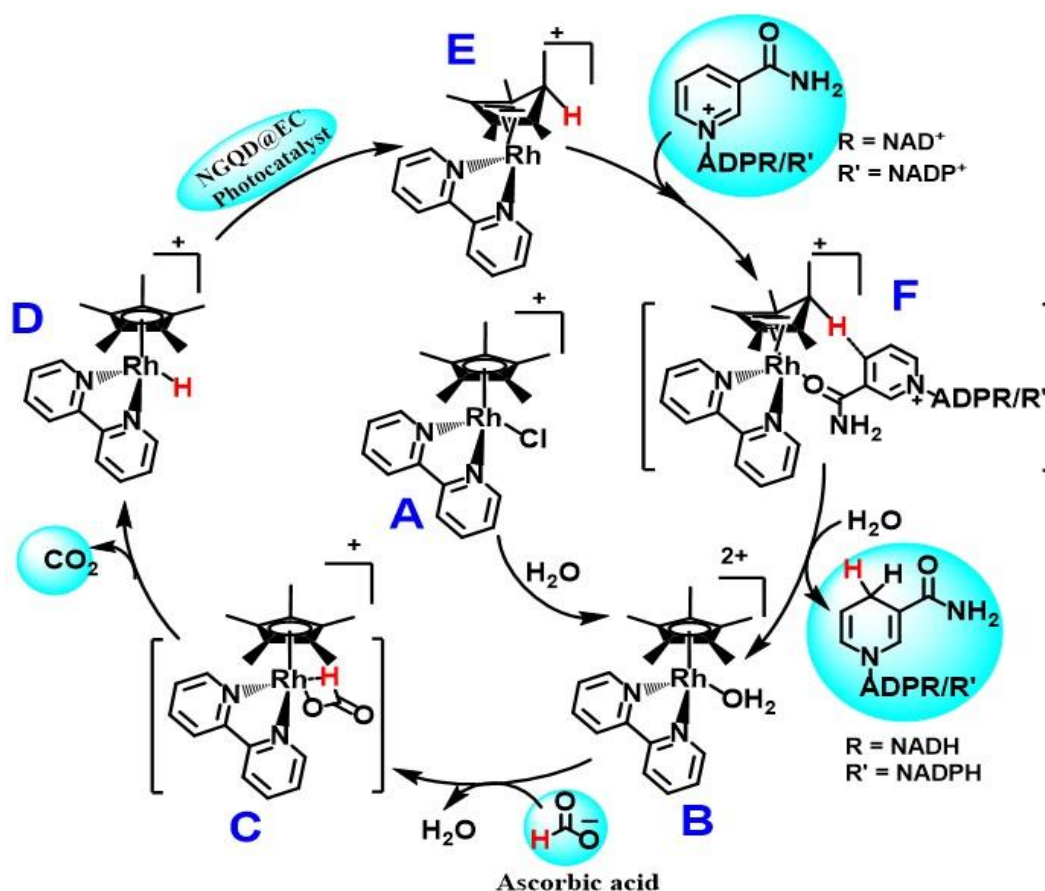
Figure 5. The negative potential graph of (a) NGQDs (−11.8 mV) and, (b) NGQDs@EC photocatalyst (−29.2 mV).



Scheme 2. Enzymatically active and inactive NADH isomer production via electrochemical reduction of NAD⁺.

2.2. Mechanistic Pathway during the Regeneration of NADH Cofactors

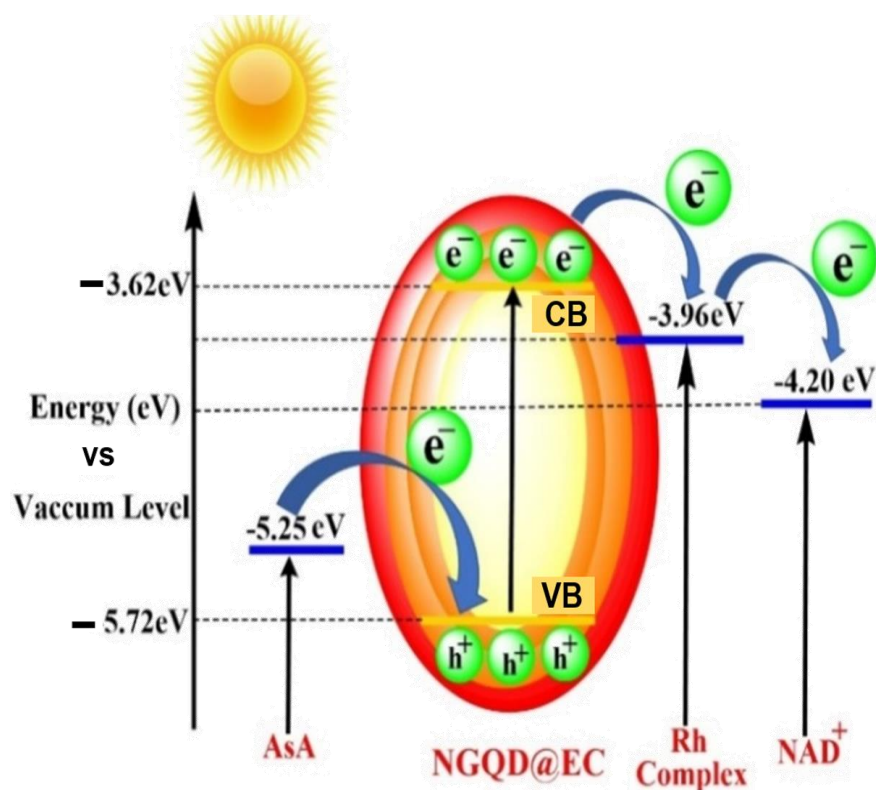
Scheme 3 depicts a mechanistic route for the rebirth of NADH cofactors. The cationic form of Rh-complex, designated as A, can be readily hydrolyzed in an aqueous buffer medium to give the water-coordinated complex $[\text{Cp}^*\text{Rh}(\text{bpy})(\text{H}_2\text{O})]^{2+}$, designated as B. The formate (HCOO^-) reacts with complex A via the hydride elimination process to produce complex B with the removal of CO_2 molecule [25]. The reduced form of complex D is formed after the supplying of charges to complex C by the photocatalyst. The rhodium hydride complex receives external electrons from the photocatalyst NGQDs@EC, resulting in the reduced intermediate D. NAD^+ can be coordinated with the D intermediate at this point, allowing hydride to be transferred to produce the regioselective NAD cofactors [26].



Scheme 3. The regeneration of NADH cofactors using NGQDs@EC photocatalyst.

2.3. Schematic Representation of Energy Level Diagram for Transfer of Photo-Excited Electron

The potential energy diagram is shown in Scheme 4. With the absorption of solar light by NGQDs@EC photocatalyst, an electron–hole pair is created in the valence band (VB). From the HOMO level (-5.72 eV) of NGQDs@EC photocatalyst to its conduction band (CB), photoexcited electrons are transferred via AsA. Thereafter, these form the LUMO (lowest unoccupied molecular orbital) level (-3.62 eV) of NGQDs@EC photocatalyst electrons transfers to NAD^+ (-4.20 eV) via rhodium complex (-3.96 eV) and lead to the regeneration of NADH. Hence, highly efficient regeneration of NADH cofactor occurs through the use of NGQDs@EC photocatalyst [24].



Scheme 4. The energy diagram shows electron generation and transfer of photoexcited electron.

2.4. Quantitative Analysis for Regeneration of NADH

As demonstrated in Figure 6, the yield (%) grew steadily in response to sun radiation. There was no yield obtained in the dark. In this experiment, product accumulation was faster, and the conversion of NAD^+ to NADH was 55% achieved in just 120 min from the NGQDs@EC photocatalyst. Therefore, the comparison of the photocatalytic performance of NGQDs and NGQDs@EC photocatalyst is important in this context. As a result, the ability of NGQDs and NGQDs@EC to photo-generate NADH under solar light was investigated, as shown in Figure 6, and an absolute increase in regeneration yield of about 55% was observed with NGQDs@EC photocatalyst compared to NGQDs under similar circumstances. As a result, a very promising production of NADH was observed with a yield percent of 55%, suggesting the huge potential of NGQDs@EC as a solar light harvesting photocatalyst [7].

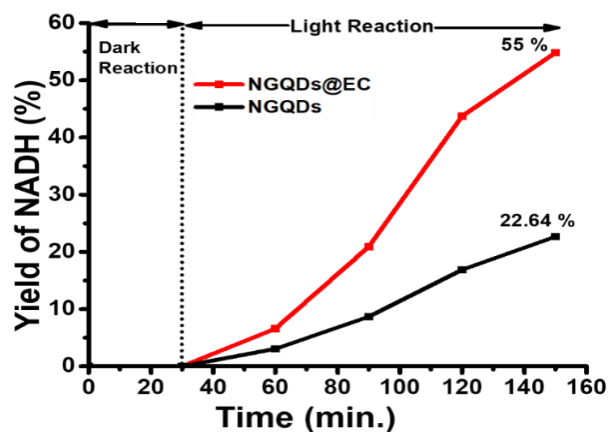


Figure 6. Regeneration of NADH from NGQDs (black line) and NGQDs@EC (red line) photocatalyst respectively.

The UV-visible performance for NADH concentration at 340 nm is studied as shown in Figure 7. Under photo-stationary circumstances, the constant rise in the absorption peak at 340 nm represents an increase in the transformation of NAD^+ to NADH over time. At 120 min, the highest conversion rate is achieved. In an artificial photosynthetic system, utilizing electron and proton transport channels, NAD^+ was reduced to NADH cofactors. [27].

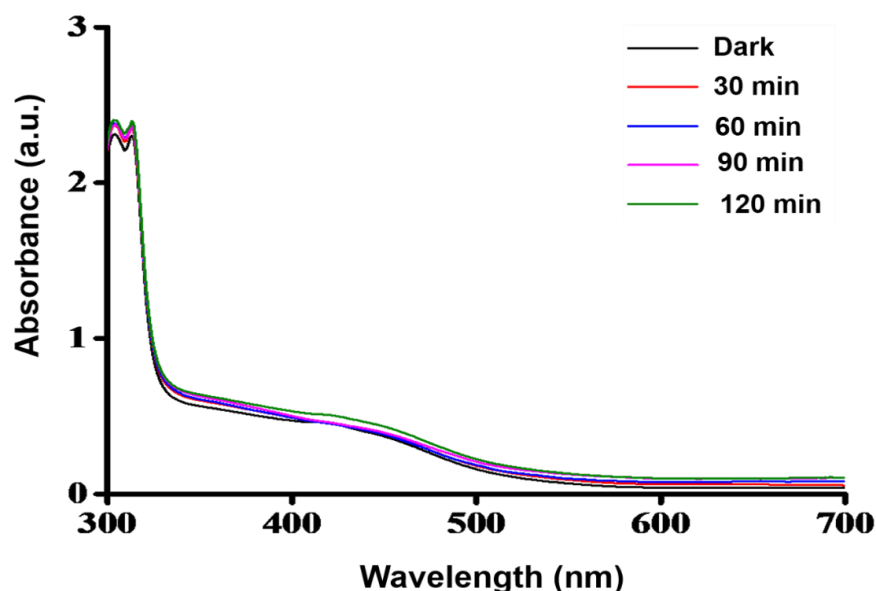


Figure 7. NGQDs@EC photocatalyst was used to record UV-visible spectroscopy for photocatalytic NADH regeneration at various time intervals.

Additionally, in Figure 8, the photostability of the NGQDs@EC photocatalyst was investigated under the same experimental conditions.

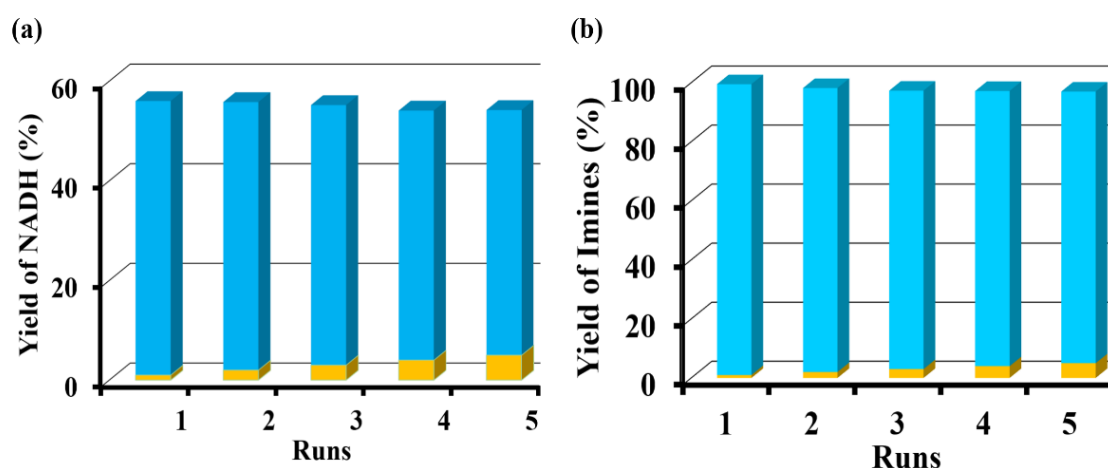


Figure 8. Photostability test of NGQDs@EC photocatalyst for (a) 1,4-NADH regeneration and, (b) Formation of Imine.

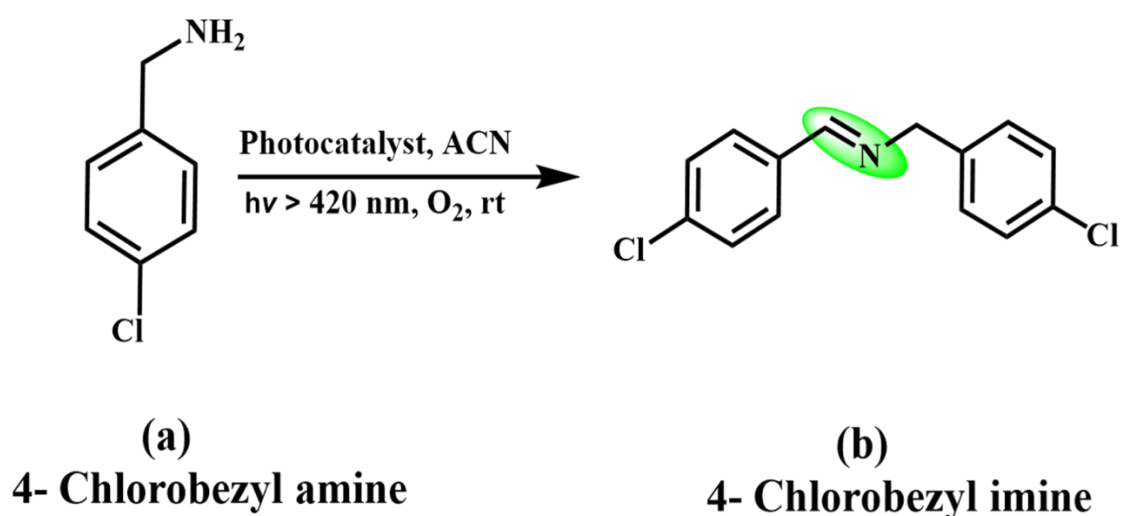
2.5. Photo-Chemically Coupling of Chlorobenzyl Amine in Presence of Oxygen

The oxidative coupling activity of the photocatalyst was screened in Table 1. When we optimized the reaction by choosing chlorobenzyl amine (125 μL) as a substrate, and NGQDs@EC (25 mg) as a photocatalyst in 10 mL ACN in the presence of O_2 under solar light, we obtained 99% yield and 99% selectivity of the product. In addition, standard reaction conditions using EC as a photocatalyst and NGQDs as a starting material provide a 33% and 28% yield of product, respectively. We have also screened the reaction in the

absence of photocatalyst, solar light, and solvent; no product was received. The result confirms that a photocatalyst, sunlight, and a solvent (acetonitrile) are essential requirements for a photocatalytic oxidative coupling reaction (Scheme 5) [28].

Table 1. Results of screening experiments.

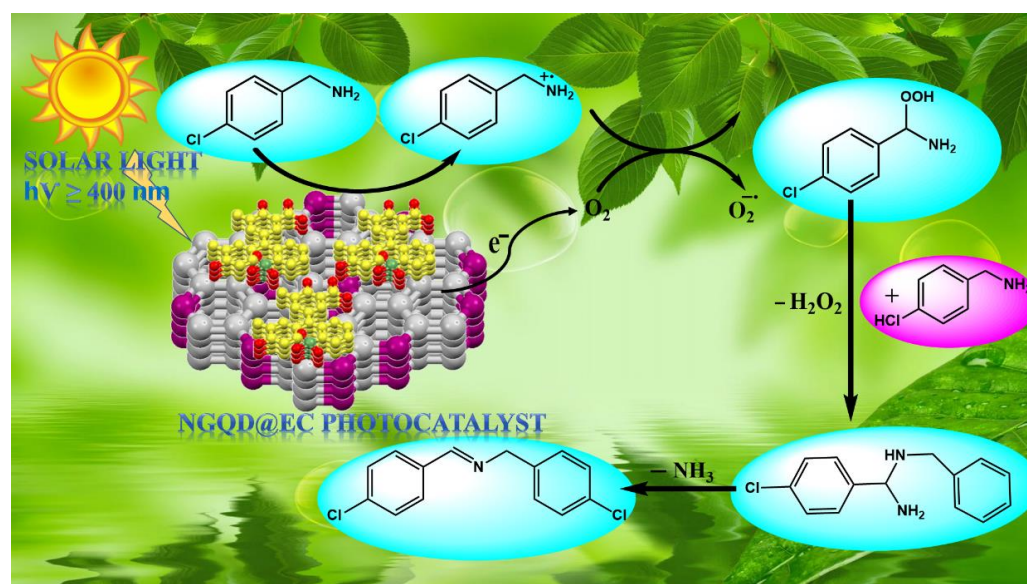
S. No.	Photocatalyst	Solvent	Solar Light	Yield (%)
1.	NGQD@EC	ACN	Yes	98.5
2.	EC	ACN	Yes	34
3.	NGQDs	ACN	Yes	12
4.	Absence	ACN	Yes	0
5.	NGQD@EC	ACN	No	5



Scheme 5. Conversion of 4-Chlorobenzyl amine (a) to 4-Chlorobenzyl imine (b).

2.6. Reaction Mechanism during the Photocatalytic Coupling Reaction

As shown in Scheme 6, the reaction is given based on the previously reported literature [26,29]. Light irradiation caused charge separation in the photocatalyst, with photogenerated electrons created in the conduction band (CB) and photogenerated holes staying in the valence band (VB). Due to its 2D planar conjugated structure, the presence of NGQDs@EC promoted charge separation and supplied electron mobility on the surface of the NGQDs@EC photocatalyst [30]. These heated electrons recombined with O_2 molecules adsorbing on the surface of NGQDs@EC, forming the O_2 radical [30]. These O_2 radicals are extremely powerful oxidizing agents, capable of converting benzylamine to imine when exposed to solar light. At the same time, due to their great oxidizing properties, reactive holes in NGQDs@EC VB can directly oxidize benzylamine molecules. As a result, the electrons and holes that have been separated are fully participating in the photocatalytic process. The NGQDs@EC photocatalyst system is utilized in a highly efficient and stereospecific solar light active manner, leading to a higher conversion of imine (98.5%) in comparison to NGQDs.



Scheme 6. The mechanistic route represents the coupling of benzylamine in the presence of oxygen and NGQDS@EC photocatalyst.

The green technology used in photocatalysis has, among its key benefits, the ability to purify water and clean the environment through solar light-induced photocatalysis. Numerous significant applications of photocatalysis exist, such as CO₂ reduction, organic pollutant degradation, removal of toxic ions and heavy metal ions, water splitting, antibacterial activity, self-cleaning process, and others. Lack of solar sensitivity and poorer efficiency are the key drawbacks of photocatalysis. The prepared NGQD@EC photocatalyst's performance was compared to that of a number of other photocatalysts that have already been published; intriguingly, it was observed that the studied NGQD@EC photocatalyst had greater photocatalytic performance compared to other published ones (Table 2). The prepared photocatalyst demonstrated outstanding photocatalytic performance, strong stability, reusability, and a highly light harvesting property.

Table 2. Comparative study of different photocatalyst for light reaction.

S.No.	Photocatalyst	NADH Regeneration (%)	Conversion of Amine (%)	References
1.	5%Ag@rGO	—————	98%	[26]
2.	CCG-BIOPY	54.02%	95%	[29]
3.	CN/BW	—————	95%	[30]
4.	CCGMAQSP	45.54%	—————	[31]
5.	NGQDs@EC	55%	98.5%	Our work

3. Experimental Details

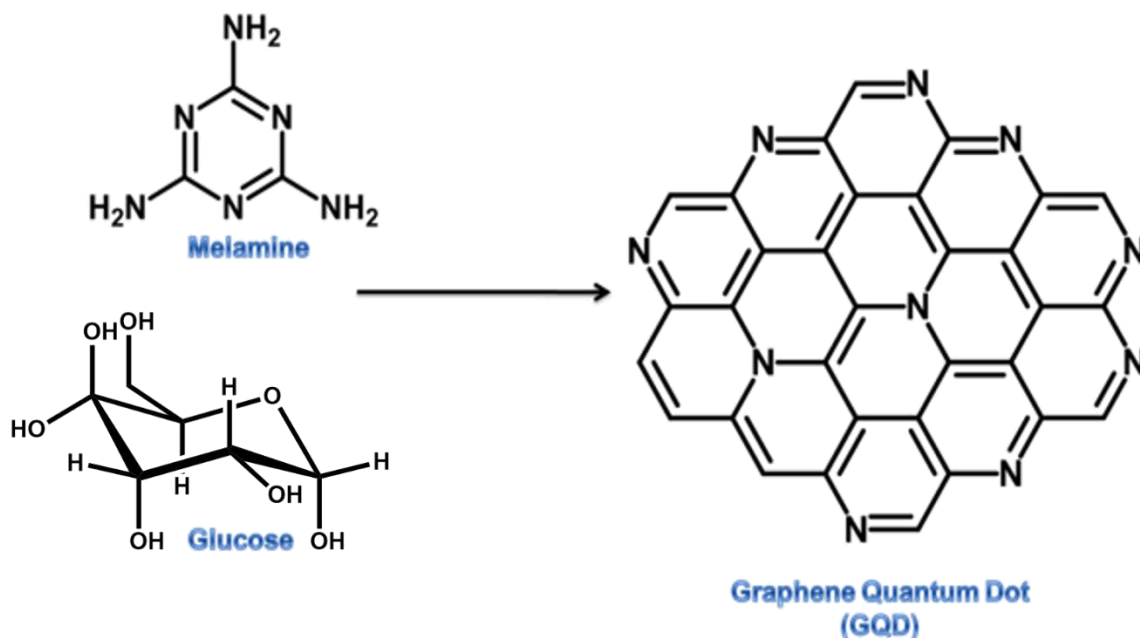
3.1. Chemicals and Materials

Graphite flakes, NAD⁺ (nicotinamide adenine dinucleotide), (Pentamethylcyclopentadienyl) rhodium (III) chloride dimer, Glucose (G), melamine (M), eriochrome cyanine (EC), ethanol (C₂H₅OH), 4-chlorobenzylamine (C₇H₈ClN) and acetonitrile (MeCN) were purchased from Sigma Aldrich and were used as received.

3.2. Synthesis of Nitrogen-Doped Graphene Quantum Dot (NGQDs)

Nitrogen-doped graphene quantum dots (NGQDs) were synthesized (Scheme 7) in a one-step process reaction. In a typical method, glucose (1 g), and melamine (4 g) were

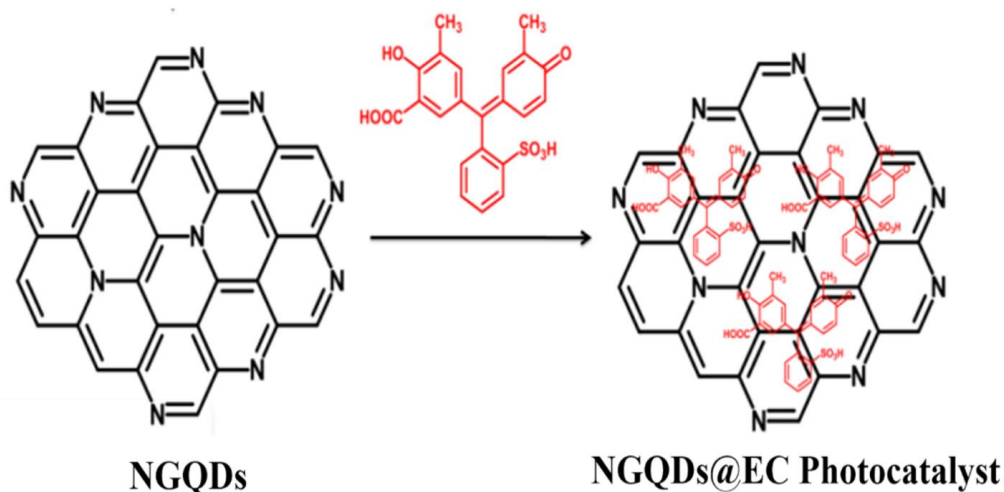
mixed together and placed in the crucible. After, that crucible was placed in the muffle furnace for 2 h at 400 °C. The compound turned from a white color into a black color; finally, nitrogen-doped graphene quantum dots were obtained [22,32].



Scheme 7. Synthesis of NGQDs₅ from Melamine and Glucose.

3.3. Synthesis of NGQDs@EC Photocatalyst

Eriochrome cyanine (750 mg) and previously prepared nitrogen-doped graphene quantum dots were dissolved in 50 mL of ethanol solution. The mixture was stirred at room temperature for 12 h and then centrifuged at 2000 rpm for 10 min. The filtrate was collected for additional analysis and photocatalysis. The compound NGQDs@EC photocatalyst was found to be 0.484 mg. The synthesis process is shown in Scheme 8 [33,34].



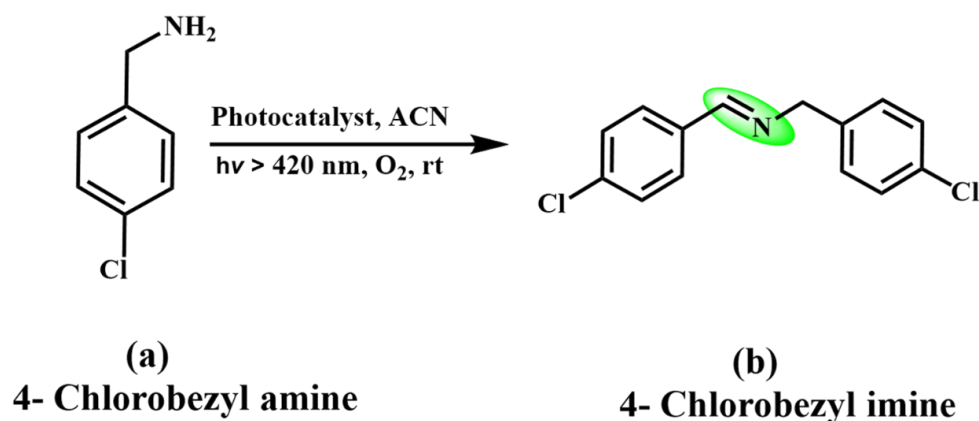
Scheme 8. Synthesis of the NGQDs@EC photocatalyst.

3.4. Photocatalytic Studies

Here, we report a self-assembled NGQDs@EC photocatalyst for 1,4-NADH regeneration, in which photoexcited electrons are rapidly pumped for NADH regeneration. Firstly, we prepared a reaction mixture for photocatalytic regeneration of 1,4-NADH. The reaction mixture contains 0.4 mM NAD^+ (248 μL), 0.2 mM electron mediator (124 μL) 0.1 M ascorbic acid (310 μL), and 10 μM NGQDs@EC photocatalyst (31 μL). Therefore, the reaction mixture was transferred to a quartz cuvette for solar light irradiation in a UV–visible spectrometer. All the ingredients were dissolved in a 0.1 M sodium phosphate buffer at pH 7.0. Then, 1,4-NADH regeneration was carried out at room temperature in a nitrogen environment. A UV–visible spectrometer was used to track the conversion in absorbance at 340 nm to quantify the photocatalytic 1,4-NADH regeneration [14,15,35].

3.5. Formation of Imine in the Presence of Oxygen

The synthesized NGQDs@EC photocatalyst was used to convert 4-chlorobenzylamine to imine due to the oxidative coupling of oxygen in the presence of solar light at room temperature. Acetonitrile was used as a solvent in the reaction medium. In the photocatalytic experiment, a 20 W white LED light was used as the light source along with a 20 mL quartz flask filled with acetonitrile (10 mL) and 4-chlorobenzylamine (125 μL), NGQDs@EC photocatalyst (25 mg). In the presence of an oxygen molecule, the resulting mixture was exposed to solar light while being stirred for 10 h. Thin layer chromatography (TLC) was used to track the progress of the reaction. The photocatalyst was separated through filtration after the reaction was completed, and the residue was concentrated under decreased pressure to get a crude product. Purification was performed using ethyl acetone column chromatography on silica gel with hexane as eluent, yielding the pure compound (shown in Scheme 9) [36].



Scheme 9. Oxidative coupling of benzylamines under solar light.

4. Conclusions

We demonstrated an eco-friendly and sustainable pathway for the production and regeneration of imine and NADH from 4-chlorobenzyl amine and NAD^+ via highly selective nitrogen-doped graphene/eriochrome cyanine composite (NGQDs@EC) photocatalyst. The NGQD@EC photocatalyst was thoroughly studied for its photocatalytic performance using UV–visible spectroscopy, FTIR spectroscopy, DSC, Zeta potential, and cyclic voltametric studies, and important, influential factors were found. Additionally, five consecutive recycle stability tests were conducted and a comparison table for the conversion and regeneration of amines and NAD^+ was compiled. This study offers a simple technique for creating benign photocatalysts that are environmentally safe and have reasonably strong photocatalytic activity for the conversion and regeneration of industrial chemicals under visible light illumination.

Author Contributions: Conceptualization, R.S., R.K.Y., R.K.S., S.S., A.P.S. and A.U.; software, R.S., R.K.Y., R.K.S., S.S., A.P.S., A.U. and N.K.G.; validation, R.S., R.K.Y., R.K.S., S.S., A.P.S., A.U. and N.K.G.; formal analysis, R.S., R.K.Y., R.K.S., S.S., A.P.S., A.U. and N.K.G.; investigation, R.S., R.K.Y., R.K.S., S.S., A.P.S., A.U. and N.K.G.; writing—original draft, R.S., R.K.Y., R.K.S., S.S., A.P.S., D.K.D. and A.U.; writing—review & editing, R.S., R.K.Y., R.K.S., S.S., A.P.S., D.K.D., A.U. and N.K.G.; visualization, D.K.D.; project administration, R.K.Y. All authors have read and agreed to the published version of the manuscript.

Funding: The authors are thankful to the Deanship of Scientific Research at Najran University, Najran, Kingdom of Saudi Arabia for funding under the Research Group funding program grant no. NU/RG/SERC/11/1.

Data Availability Statement: No Supplementary data is available.

Acknowledgments: Authors are thankful to MMMUT, Gorakhpur-273010, U. P., India for providing the platform for research. The authors are thankful to the Deanship of Scientific Research at Najran University, Najran, Kingdom of Saudi Arabia for funding under the Research Group funding program grant no. NU/RG/SERC/11/1.

Conflicts of Interest: The authors declare no competing financial interests.

References

1. Yasuhiro, T.; Vayssieres, L.; Durrant, J. Artificial photosynthesis for solar water-splitting. *Nat. Photonics* **2012**, *6*, 511–518.
2. Serena, B.; Drouet, S.; Francà, L.; Gimbert-Suriñach, C.; Guttentag, M.; Richmond, C.; Stoll, T.; Llobet, A. Molecular artificial photosynthesis. *Chem. Soc. Rev.* **2014**, *43*, 7501–7519.
3. Osterloh, F.E. Inorganic Materials as Catalysts for Photochemical Splitting of Water. *Chem. Mater.* **2008**, *20*, 35–54. [[CrossRef](#)]
4. Wang, X.; Saba, T.; Yiu, H.H.P.; Howe, R.; Anderson, J.; Shi, J. Cofactor NAD(P)H regeneration inspired by heterogeneous pathways. *Chem* **2017**, *2*, 621–654. [[CrossRef](#)]
5. Liu, J.; Antonietti, M. Bio-inspired NADH regeneration by carbon nitride photocatalysis using diatom templates. *Energy Environ. Sci.* **2013**, *6*, 1486–1493. [[CrossRef](#)]
6. Huang, J.; Antonietti, M.; Liu, J. Bio-inspired carbon nitride mesoporous spheres for artificial photosynthesis: Photocatalytic cofactor regeneration for sustainable enzymatic synthesis. *J. Mater. Chem. A* **2014**, *2*, 7686–7693. [[CrossRef](#)]
7. Gupta, S.K.; Yadav, R.; Gupta, A.; Yadav, B.; Singh, A.; Pande, B. Highly Efficient S-g-CN/Mo-368 Catalyst for Synergistically NADH Regeneration Under Solar Light. *Photochem. Photobiol.* **2021**, *97*, 1498–1506. [[CrossRef](#)]
8. Yang, D.; Zou, H.; Wu, Y.; Shi, J.; Zhang, S.; Wang, X.; Han, P.; Tong, Z.; Jiang, Z. Constructing quantum dots@flake g-C₃N₄ isotype heterojunctions for enhanced visible-light-driven NADH regeneration and enzymatic hydrogenation. *Ind. Eng. Chem. Res.* **2017**, *56*, 6247–6255. [[CrossRef](#)]
9. Wan, J.; Choi, W.; Kim, J.; Kuk, S.; Lee, S.; Park, C. Self-Assembled Peptide-Carbon Nitride Hydrogel as a Light-Responsive Scaffold Material. *Biomacromolecules* **2017**, *18*, 3551–3556.
10. Shifa, T.A.; Wang, F.; Liu, Y.; He, J. Heterostructures Based on 2D Materials: A Versatile Platform for Efficient Catalysis. *Adv. Mater.* **2019**, *31*, 1804828. [[CrossRef](#)]
11. Iyer, M.S.K.; Patil, S.; Singh, A. Flame Synthesis of Functional Carbon Nanoparticles. *Trans. Indian Natl. Acad. Eng.* **2022**, *7*, 787–807. [[CrossRef](#)]
12. Kang, H.; Liu, H.; Li, C.; Sun, L.; Zhang, C.; Gao, H.; Yin, J.; Yang, B.; You, Y.; Jiang, K.; et al. Polyanthraquinone-Triazine—A Promising Anode Material for High-Energy Lithium-Ion Batteries. *ACS Appl. Mater. Interfaces* **2018**, *10*, 37023–37030. [[CrossRef](#)] [[PubMed](#)]
13. Chaubey, S.; Yadav, R.; Tripathi, S.K.; Yadav, B.; Singh, S.; Kim, T.W. Covalent Triazine Framework as an Efficient Photocatalyst for Regeneration of NAD(P)H and Selective Oxidation of Organic Sulfide. *Photochem. Photobiol.* **2022**, *98*, 150–159. [[CrossRef](#)] [[PubMed](#)]
14. Singh, S.; Yadav, R.; Kim, T.; Singh, C.; Singh, P.; Singh, A.; Singh, A.; Singh, A.; Beag, J.; Gupta, S. Rational design of a graphitic carbon nitride catalytic–biocatalytic system as a photocatalytic platform for solar fine chemical production from CO₂. *React. Chem. Eng.* **2022**, *7*, 1566–1572. [[CrossRef](#)]
15. Singh, P.; Yadav, R.; Kim, T.; Yadav, T.; Gole, V.; Gupta, A.; Singh, K.; Kumar, K.; Yadav, B.; Dwivedi, D. Solar light active flexible activated carbon cloth-based photocatalyst for Markovnikov-selective radical-radical cross-coupling of S-nucleophiles to terminal alkyne and liquefied petroleum gas sensing. *J. Chin. Chem. Soc.* **2021**, *68*, 1435–1444. [[CrossRef](#)]
16. Pan, D.; Zhang, J.; Li, Z.; Wu, M. Hydrothermal Route for Cutting Graphene Sheets into Blue-Luminescent Graphene Quantum Dots. *Adv. Mater.* **2010**, *22*, 734–738. [[CrossRef](#)]
17. Li, Y.; Hu, Y.; Zhao, Y.; Shi, G.; Deng, L.; Hou, Y.; Qu, L. An electrochemical avenue to green-luminescent graphene quantum dots as potential electron-acceptors for photovoltaics. *Adv. Mater.* **2011**, *23*, 776–780. [[CrossRef](#)]
18. Chen, J.; Collier, C. Noncovalent Functionalization of Single-Walled Carbon Nanotubes with Water-Soluble Porphyrins. *J. Phys. Chem. B* **2005**, *109*, 7605–7609. [[CrossRef](#)]

19. Li, B.; Cao, H.; Yin, G.; Lu, Y.; Yin, J. Facile synthesis of silver@graphene oxide nanocomposites and their enhanced antibacterial properties. *J. Mater. Chem.* **2011**, *21*, 13765–13768. [[CrossRef](#)]
20. Silva, S.P.; Moraes, D.; Samios, D. Iron Oxide Nanoparticles Coated with Polymer Derived from Epoxidized Oleic Acid and Cis-1,2-Cyclohexanedicarboxylic Anhydride: Synthesis and Characterization. *J. Mater. Sci. Eng.* **2016**, *5*, 1000247. [[CrossRef](#)]
21. Wang, J.; Lu, C.; Chen, T.; Hu, L.; Du, Y.; Yao, Y.; Goh, M. Simply synthesized nitrogen-doped graphene quantum dot (NGQD)-modified electrode for the ultrasensitive photoelectrochemical detection of dopamine. *Nanophotonics* **2020**, *9*, 3831–3839. [[CrossRef](#)]
22. Chaubey, S.; Singh, P.; Singh, C.; Singh, S.; Shreya, S.; Yadav, R.; Mishra, S.; Jeong, Y.-J.; Biswas, B.; Kim, T. Ultra-efficient synthesis of bamboo-shape porphyrin framework for photocatalytic CO₂ reduction and consecutive C-S/C-N bonds formation. *J. CO₂ Util.* **2022**, *59*, 101968. [[CrossRef](#)]
23. Cimino, P.; Troiani, A.; Pepi, F.; Garzoli, S.; Salvitti, C.; Di Rienzo, B.; Barone, V.; Ricci, A. From ascorbic acid to furan derivatives: The gas phase acid catalyzed degradation of vitamin C. *Phys. Chem. Chem. Phys.* **2018**, *20*, 17132–17140. [[CrossRef](#)]
24. Singh, C.; Yadav, R.; Kim, T.; Baeg, J.-O.; Singh, A. Greener One-step Synthesis of Novel In Situ Selenium-doped Framework Photocatalyst by Melem and Perylene Dianhydride for Enhanced Solar Fuel Production from CO₂. *Photochem. Photobiol.* **2022**, *98*, 998–1007. [[CrossRef](#)]
25. Yadav, R.K.; Oh, G.; Park, N.; Kumar, A.; Kong, K.; Baeg, J. Highly selective solar-driven methanol from CO₂ by a photocatalyst/biocatalyst integrated system. *J. Am. Chem. Soc.* **2014**, *136*, 16728–16731. [[CrossRef](#)]
26. Kumar, A.; Sadanandhana, A.M.; Jain, S.L. Silver doped reduced graphene oxide as promising plasmonic photocatalyst for oxidative coupling of benzylamines under visible light irradiation. *New J. Chem.* **2019**, *43*, 9116–9122. [[CrossRef](#)]
27. Bajorowicz, B.; Reszczyńska, J.; Lisowski, W.; Klimczuk, T.; Winiarski, M.; Słoma, M.; Zaleska-Medynska, A. Perovskite-type KTaO₃-reduced graphene oxide hybrid with improved visible light photocatalytic activity. *RSC Adv.* **2015**, *5*, 91315–91325. [[CrossRef](#)]
28. Feng, Y.; Wang, G.; Liao, J.; Li, W.; Chen, C.; Li, M.; Li, Z. Honeycomb-like ZnO Mesoporous Nanowall Arrays Modified with Ag Nanoparticles for Highly Efficient Photocatalytic Activity. *Sc. Rep.* **2017**, *7*, 11622. [[CrossRef](#)]
29. Yadav, R.K.; Baeg, J.-O.; Kumar, A.; Kong, K.; Oh, G.; Park, N.-J. Graphene-BODIPY as a photocatalyst in the photocatalytic-biocatalytic coupled system for solar fuel production from CO₂. *J. Mater. Chem.* **2014**, *2*, 5068–5076. [[CrossRef](#)]
30. Yuan, A.; Lei, H.; Wang, Z.; Dong, X. Improved photocatalytic performance for selective oxidation of amines to imines on graphitic carbon nitride/bismuth tungstate heterojunctions. *J. Colloid Interface Sci.* **2020**, *560*, 40–49. [[CrossRef](#)]
31. Yadav, R.K.; Baeg, J.-O.; Oh, G.; Park, N.-J.; Kong, K.; Kim, J.; Hwang, D.W.; Biswas, S.K. A Photocatalyst–Enzyme Coupled Artificial Photosynthesis System for Solar Energy in Production of Formic Acid from CO₂. *J. Am. Chem. Soc.* **2012**, *134*, 11455–11461. [[CrossRef](#)]
32. Liu, F.; Huang, K.; Ding, S.; Dai, S. One-step synthesis of nitrogen-doped graphene-like meso-macroporous carbons as highly efficient and selective adsorbents for CO₂ capture. *J. Mater. Chem. A* **2016**, *4*, 14567–14571. [[CrossRef](#)]
33. Zhang, K.; Li, H.; Shi, H.; Hong, W. Polyimide with enhanced π stacking for efficient visible-light-driven photocatalysis. *Catal. Sci. Technol.* **2021**, *11*, 4889–4897. [[CrossRef](#)]
34. Mou, Z.; Dong, Y.; Li, S.; Du, Y.; Wang, X.; Yang, P.; Wang, S. Eosin Y functionalized graphene for photocatalytic hydrogen production from water. *Int. J. Hydrogen Energy* **2011**, *36*, 8885–8893. [[CrossRef](#)]
35. Singh, S.; Yadav, R.; Kim, T.; Singh, C.; Singh, P.; Chaubey, S.; Singh, A.; Baeg, J.; Gupta, S.; Tiwary, D. Generation and Regeneration of the C(sp³)-F Bond and 1,4-NADH/NADPH via Newly Designed S-gC₃N₄@Fe₂O₃/LC Photocatalysts under Solar Light. *Energy Fuels* **2022**, *36*, 8402–8412. [[CrossRef](#)]
36. Kumar, A.; Hamdi, A.; Coffinier, Y.; Addad, A.; Roussel, P.; Boukherroub, R.; Jain, S. Visible light assisted oxidative coupling of benzylamines using heterostructured nanocomposite photocatalyst. *Chemistry* **2018**, *356*, 457–463. [[CrossRef](#)]

Disclaimer/Publisher’s Note: The statements, opinions and data contained in all publications are solely those of the individual author(s) and contributor(s) and not of MDPI and/or the editor(s). MDPI and/or the editor(s) disclaim responsibility for any injury to people or property resulting from any ideas, methods, instructions or products referred to in the content.